

Evidence of local effects in anomalous refraction and focusing properties of dodecagonal photonic quasicrystals

Emiliano Di Gennaro,* Carlo Miletto, Salvatore Savo, and Antonello Andreone
CNISM and Department of Physics, University of Naples "Federico II", Piazzale Tecchio 80, I-80125 Naples, ITALY

Davide Morello, Vincenzo Galdi, Giuseppe Castaldi, and Vincenzo Pierro
*Waves Group, Department of Engineering, University of Sannio,
Corso Garibaldi 107, I-82100 Benevento, ITALY*
(Dated: October 27, 2018)

We present the key results from a comprehensive study of the refraction and focusing properties of a two-dimensional dodecagonal photonic “quasicrystal” (PQC), carried out via both full-wave numerical simulations and microwave measurements on a slab made of alumina rods inserted in a parallel-plate waveguide. We observe anomalous refraction and focusing in several frequency regions, confirming some recently published results. However, our interpretation, based on numerical and experimental evidence, differs substantially from the one in terms of “effective negative refractive-index” that was originally proposed. Instead, our study highlights the critical role played by short-range interactions associated with local order and symmetry.

PACS numbers: 42.70.Qs, 41.20.Jb, 61.44.Br, 42.30.-d

Since the pioneering work by Yablonovitch¹ and John², “photonic crystals” (PCs) have elicited great attention from the scientific community, in view of the variety of peculiar electromagnetic (EM) bandgap, waveguiding/confinement, refraction, and emission effects attainable through their use. Among the most intriguing applications, it is worth mentioning those to negative refraction and subwavelength imaging (“superlensing”)^{3,4,5,6}. The most typical PC configurations are based on dielectric inclusions (or voids) arranged according to *periodic* lattices in a host medium, and can thus be studied using well-established tools and concepts such as Bloch theorem, unit cell, Brillouin zone, equifrequency surfaces, etc.

With specific reference to lensing applications, two different approaches have been presented to obtain subwavelength resolution using a dielectric PC slab. In the first one, a PC with high dielectric contrast is tuned so as to behave (usually near a frequency band edge) like a homogeneous material with a negative refractive index $n = -1^3$, and the focus position of the flat lens follows a simple ray-optical construction⁷. In the second approach, “all angle negative refraction” (AANR) is achieved without an effective negative index, provided that the equifrequency surfaces (EFSs) of the PC are all convex and larger than the one pertaining to the host medium⁸. In this case, the focus position does not follow the ray-optical construction and is *restricted*⁹.

During the last decade, the discovery in solid-state physics of certain metallic alloys (the so-called “quasicrystals”^{10,11}) whose X-ray diffraction spectra exhibit “noncrystallographic” rotational symmetries (e.g., 5-fold or ($K > 6$)-fold, known to be incompatible with spatial periodicity) has generated a growing interest toward *aperiodically-ordered* geometries, leading to the study of the so-called “photonic quasicrystals” (PQCs). In this framework, useful tools for geometrical parameterization can be borrowed from the theory of “aperi-

odic tilings”¹². Several recent numerical and experimental studies have explored the EM properties of PQCs, in the form of two-dimensional (2-D) aperiodic arrays of cylindrical rods or holes, as well as 3-D structures fabricated via stereolithography (see 13 and the references therein for a recent review of the subject).

The study of PQCs entails significant complications, from both theoretical and computational viewpoints, as compared to standard (periodic) PCs. In spite of the lack of the aforementioned Bloch-type concepts and tools, approaches to the calculation of the density of states in PCQs have been proposed, relying, e.g., on rational approximants^{14,15} or on extended zone schemes in the reciprocal space¹⁶. However, many PQC properties and underlying mechanisms, which generally involve short- and long-range interactions as well as complex multiple scattering phenomena, are not yet fully understood. Nevertheless, results have revealed the possibility of obtaining similar properties as those exhibited by periodic PCs, with interesting potentials (e.g., richer bandgap structure with lower and/or multiple frequencies of operation, higher isotropy, easier achievement of phase-matching conditions, etc.) in view of the additional degrees of freedom typically available in aperiodically-ordered structures.

Recently, some examples of 2-D PQCs characterized by high-order (8-fold, 10-fold, and 12-fold) rotational symmetries have been proposed as good candidates to exhibit negative refraction and subwavelength focusing effects with polarization-insensitive and non-near-field imaging capabilities^{17,18}. Similar results were also obtained in case of acoustic waves¹⁹. Such effects and properties were interpreted in 17 within the framework of “effective negative refractive-index and evanescent wave amplification.”

In this letter, we present the key results from a comprehensive study, based on full-wave numerical simulations backed by experimental verifications, which show that

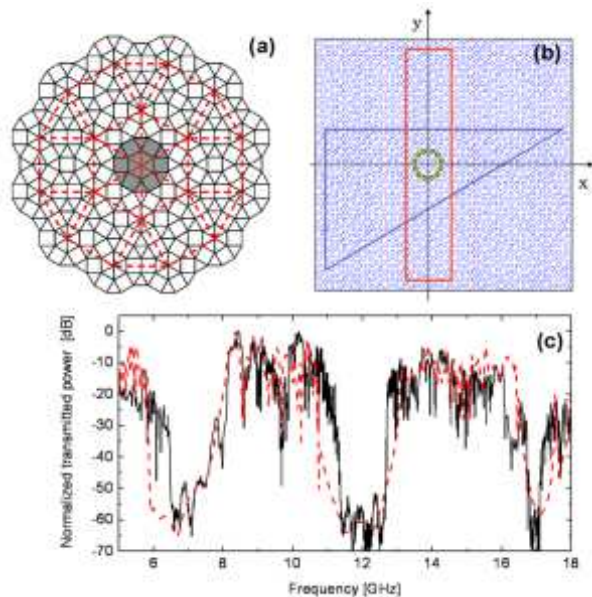


FIG. 1: (color online) (a): Illustration of the Stampfli inflation rule. Starting from the parent tiling represented by the gray-shaded central dodecagon, a big parent (red dashed lines) is generated by inflation, and filled up with copies of the original dodecagon placed at its vertices. (b): A portion of the tiling with the slab ($\sim 7a$ thickness) and wedge realizations considered in 17 (as well as in our study) marked by red and blue solid contours, respectively. The green-full-dot dodecagon corresponds to the parent tiling shown in (a). (c): Comparison (in a normalized scale) between the measured (black continuous curve) and simulated (red dashed curve) transmitted power for the PQC slab in (b) with $a = 1.33$ cm.

the “effective negative refractive-index” interpretation is questionable and unable to fully explain and predict the above effects, which instead arise from complex near-field scattering effects and short-range interactions critically associated to local symmetry points in the PQC.

The PQC of interest is a conformally-scaled version of that in 17, made of dielectric alumina rods (relative permittivity $\epsilon_r = 8.6$) of radius $r = 0.4$ cm placed (in air) at the vertices of a square-triangle 12-fold-symmetric tiling with lattice constant (tile sidelength) $a = 1.33$ cm, generated according to the Stampfli recursive construction²⁰ (see also Fig. 1a). Figure 1b illustrates two particular slab- and wedge-shaped tiling cuts (as in 17) considered in our study.

In our numerical simulations, assuming the rods infinitely long and parallel to the electric field, we employ a well-established full-wave technique (based on Bessel-Fourier multipolar expansion²¹), which has been extensively applied to the study of 2-D finite-size PCs²² and PQCs²³. The experimental verification relies on microwave (X-band) measurements on PCQ slabs made of alumina rods of height $h = 1$ cm inserted in an aluminum parallel-plate waveguide terminated with microwave absorbers, with a monopole antenna used to generate an

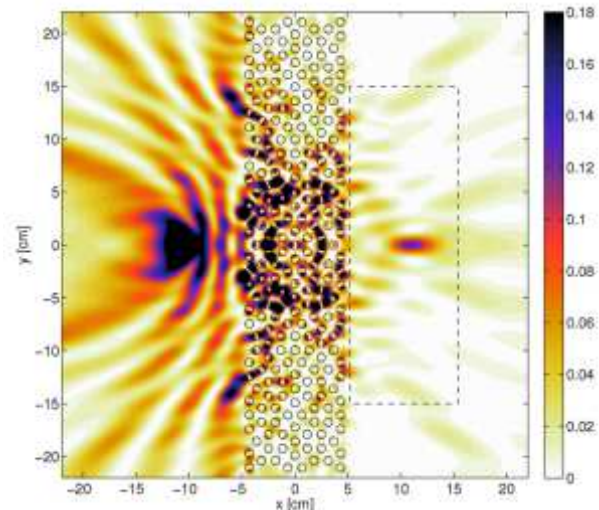


FIG. 2: (color online) Simulated field intensity map at 8.836 GHz for a PQC slab as in Fig. 1c (with lateral width of 42.9 cm and thickness of 9.4 cm), illustrating the focusing of a source placed at $y_s = 0$ and at a distance $d_x = 6$ cm from the slab surface. The dashed rectangle delimits the 10cm \times 30cm area scanned in the image-side measurements.

electric field parallel to the rods. The intensity/phase maps are collected using a HP8720C Vector Network Analyzer and a computer-controlled $x-y$ movable monopole antenna probe, in a setup similar to that described in 5,24.

As a preliminary check, we studied the transmission properties of the PQC slab in Fig. 1b, for a fixed source position, within the 5 – 18GHz frequency range. Figure 1c compares the experimental and simulated (normalized) transmitted power through the slab. Three main bandgap regions are clearly observed, with fairly good agreement between simulations and measurements. We then studied the focusing properties within the frequency region 8 – 10 GHz (between the first and second bandgaps), by observing the field intensity maps at the image side. We found several frequency regions (including those reported in 17) where a clear focus was visible, with bandwidth ranging from few to thousands MHz. We note that this feature represents a first remarkable difference with the (periodic) PC case, where the focusing regions tend to be more rare and well separated. The seemingly *denser* occurrence of focusing effects in PQCs could be attributed to their inherent self-similar nature²⁵. We observed the most stable focusing effects around 8.350 GHz. However, in what follows we concentrate on the focusing effects at 8.836 GHz, corresponding to the configuration considered in 17. In our study emphasis is not placed on *quantitative* assessments of the subwavelength focusing capabilities, but rather on the phenomenology interpretation, and its similarities and differences with respect to the periodic PC case.

Figure 2 shows an example of a field intensity map in-

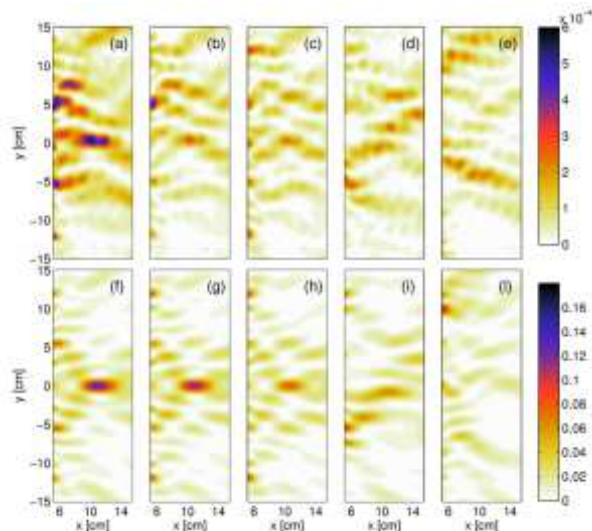


FIG. 3: (color online) As in Fig. 2, but details of the measured (a–e) and simulated (f–l) field intensity maps at the image side, for various source positions. (a), (f): Source at $y_s = 0$, and at a distance $d_x = 6$ cm from the slab surface (cf. Fig. 2); (b), (g): $y_s = 0$ and $d_x = 7$ cm; (c), (h): $y_s = 0$ and $d_x = 8$ cm; (d), (i): $y_s = 1$ cm and $d_x = 6$ cm; (e), (l): $y_s = 5$ cm and $d_x = 6$ cm.

side and outside the PQC slab in Fig. 1b. It is worth noticing that such slab is centered at the center of the tiling ($x = y = 0$, see Fig. 1b), which is not only a center of local (12-fold) rotational symmetry, but also possesses reflection symmetries with respect to both x and y axes. The presence of a focus at the image side is clearly observed. However, from a comprehensive numerical parametric study (see also 26 for more details), we found that neither a ray diagram approach can be used nor a preferential propagation direction can be established to justify and predict the image formation. Conversely, we found that a local structure (in particular, the green-full-dot dodecagon parent tiling highlighted in Fig. 1b) around the local symmetry center plays a key role.

If the PQC slab behaved like a homogeneous material with a negative refractive index $n = -1$, the source-image distance would remain constant and equal to twice the slab thickness⁷. Results for periodic PCs showing an almost isotropic refractive response (see, e.g., 9) agree fairly well with this prediction. Moreover, in PC lenses, for lateral displacements of the source that preserve the distance from the lens interface as well as the structure periodicity, the focus remains unaffected, and its position follows the source location, in view of the absence of an optical axis.

Figure 3 shows some representative measured and simulated field intensity maps at the image side of the PQC slab, for orthogonal and parallel (to the slab interface) displacements of the source. Again, a general good agreement is observed between simulations and measurements. Specifically, Figs. 3a and 3f pertain to the configuration

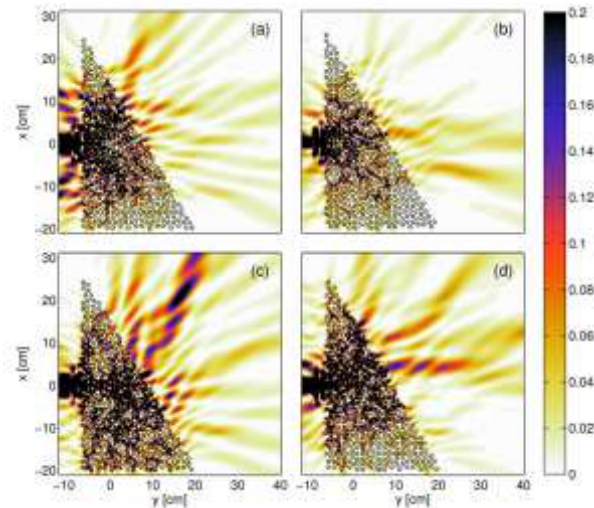


FIG. 4: (color online) Simulated intensity field maps at 8.836 GHz for a collimated Gaussian beam (with minimum spot-size ~ 2.8 cm) normally impinging on several realizations of a PQC 60°-wedge. (a): Incident beam axis intersecting the local symmetry center, as in 17[Fig. 2]. (b)–(d): Different wedge realizations obtained by random rigid translations of the tiling (so as to displace the local symmetry center from the incident beam axis).

in Fig. 2, whereas Figs. 3b, 3g and Figs. 3c, 3h pertain to source displacements along the x -axis (i.e., orthogonal to the slab interface), which preserve the $y_s = 0$ position (i.e., keeping the source facing the local symmetry center of the tiling). The focus position does not change substantially, raising further concerns about the interpretation in 17. Moving the source parallel to the slab surface, and therefore breaking the symmetry around the x -axis, one observes from Figs. 3d, 3i and Figs. 3e, 3l that even small displacements significantly affect the focus image, which undergoes a rapid deterioration until it completely disappears for the source placed at $y_s = 5$ cm. Interestingly, a focus can be still observed as long as one extends the slab size along the y -axis and places the source at $y_s = 13.67$ cm, i.e., directly facing the symmetry center of another big parent tiling (see Fig.1b). In this case, however, the image (not shown for brevity) exhibits a worse quality. The complex interplay between local and global order and symmetry in the focusing properties, which can be glanced from the above results, is confirmed by parametric studies of PQC slabs of different thicknesses, where a variety of effects can be observed, ranging from localized (single and multiple) spots to beaming phenomena (see 26 for details).

As a further check, we also carried out a numerical study involving a collimated Gaussian beam impinging with normal incidence on the surface of PQC 60°-wedges extracted from the dodecagonal tiling. Results are shown in Fig. 4. Specifically, Fig. 4a pertains to the wedge realization shown in Fig. 1b, with the incident beam

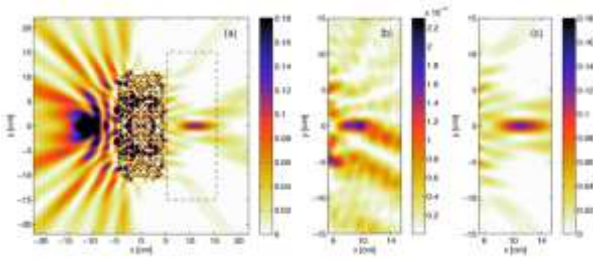


FIG. 5: (color online) (a): As in Fig. 2, but for a PQC slab with lateral width reduced to 22cm. (b), (c): Details of the measured and simulated field intensity maps, respectively, at the image side.

axis intersecting the local symmetry center. Again, our results are similar to those in 17, with the transmitted beam propagating mainly in the “negative” direction – a phenomenon previously interpreted within the framework of “effective negative refractive-index.” However, a deeper study reveals that this effect too is critically related to the mutual position of the incident beam and the local symmetry center. This is clearly visible in Figs. 4b–4d, pertaining to different PQC wedge samples obtained by random rigid translations of the tiling (so as to displace the local symmetry center from the incident beam axis), which display complex multi-beam features in the transmitted field, thereby highlighting the absence of a clear-cut refractive behavior.

From the above results, which confirm the key role played by *short range* interactions involving a neighborhood of the parent tiling, one could speculate that the focusing properties of a PQC slab would be restricted to a limited range of incidence angles, and should therefore occur also for significantly reduced lateral widths. Indeed, the focusing effects turn out to be rather *robust* with respect to lateral width reductions that do not affect

significantly the modal field distribution in a neighboring region of the local symmetry center. Figure 5 shows the simulated and experimental results pertaining to a PQC slab with lateral width of only 22cm (i.e., \sim six wavelengths, nearly half of that in Fig. 2), and yet still exhibiting a clear focus. Similar results were also obtained for PQC slabs with even smaller (only three wavelengths) lateral width, but with larger thickness²⁶.

In conclusion, our numerical and experimental study of the refraction and focusing properties of dodecagonal PQCs confirms some of the results reported in the recent literature¹⁷, but shows that, contrary to the original interpretation, such results are not attributable to an “effective negative refractive-index.” Instead, they arise from complex near-field scattering effects and short-range interactions critically associated to local symmetry points in the PQC, which were only glossed over in previous studies. In this connection, it is worth recalling that local order and symmetry have already been observed to play a key role in a variety of PQC-related effects, including bandgap formation²³, field localization²⁷, and directive emission²⁸. The new evidence and insights presented in this letter constitute a further step toward a full understanding of the underlying mechanisms, which remains crucial for their judicious exploitation in the design of novel *compact* optical systems. Within this framework, further numerical and experimental studies of various PQC geometries are worth pursuing.

Acknowledgments

This work has been funded by the Italian Ministry of Education and Scientific Research (MIUR) under the PRIN-2006 grant on “Study and realization of metamaterials for electronics and TLC applications.”

* emiliano@na.infn.it

¹ E. Yablonovitch, Phys. Rev. Lett. **58**, 2059 (1987).
² S. John, Phys. Rev. Lett. **58**, 2486 (1987).
³ M. Notomi, Phys. Rev. B **62**, 10696 (2000).
⁴ S. Foteinopoulou and C. M. Soukoulis, Phys. Rev. B **72**, 165112 (2005).
⁵ P. Parimi *et al.*, Nature (London) **426**, 404 (2003).
⁶ E. Cubukcu *et al.*, Nature (London) **423**, 604 (2003).
⁷ W. T. Lu and S. Sridhar, Optics Express **13**, 10673 (2005).
⁸ C. Luo *et al.*, Phys. Rev. B **68**, 045115 (2003).
⁹ Y. Wang *et al.*, Phys. Rev. B **68**, 165106 (2003).
¹⁰ D. Shechtman *et al.*, Phys. Rev. Lett. **53**, 1951 (1984).
¹¹ D. Levine and P. J. Steinhardt, Phys. Rev. Lett. **53**, 2477 (1984).
¹² M. Senechal, *Quasicrystals and Geometry* (Cambridge University Press, Cambridge, UK, 1995).
¹³ W. Steurer and D. Sutter-Widmer, J. Phys. D: Appl. Phys. **40**, R229 (2007).
¹⁴ A. E. Carlsson, Phys. Rev. B **47**, 2515 (1993).

¹⁵ S. David *et al.*, IEEE J. Quantum Elect. **37**, 1427 (2001).
¹⁶ M. A. Kaliteevski *et al.*, J. Phys.: Condens. Matter **13**, 10459 (2001).
¹⁷ Z. Feng *et al.*, Phys. Rev. Lett. **94**, 247402 (2005).
¹⁸ X. Zhang *et al.*, Optics Express **15**, 1292 (2007).
¹⁹ X. Zhang, Phys. Rev. B **75**, 024209 (2007).
²⁰ M. Oxborrow and C. L. Henley, Phys. Rev. B **48**, 6966 (1993).
²¹ D. Felbacq *et al.*, J. Opt. Soc. Am. A **11**, 2526 (1994).
²² A. Asatryan *et al.*, Phys. Rev. E **63**, 046612 (2001).
²³ A. Della Villa *et al.*, Phys. Rev. Lett. **94**, 183903 (2005).
²⁴ P. Parimi *et al.*, Phys. Rev. Lett. **92**, 127401 (2004).
²⁵ M. A. Kaliteevski *et al.*, J. Mod. Opt. **47**, 1771 (2000).
²⁶ E. Di Gennaro *et al.*, to be published in Photonics and Nanostructure: Fundamentals and Applications (2008), arXiv:0711.4239v1 [physics.optics].
²⁷ A. Della Villa *et al.*, Optics Express **14**, 10021 (2006).
²⁸ A. Micco *et al.*, arXiv:0711.3097v1 [physics.optics] (2007).